A second-order continuity domain-decomposition technique based on integrated Chebyshev polynomials for two-dimensional elliptic problems

N. Mai-Duy* and T. Tran-Cong

Computational Engineering and Science Research Centre (CESRC)

Faculty of Engineering and Surveying

The University of Southern Queensland, Toowoomba, QLD 4350, Australia

Submitted to *Applied Mathematical Modelling*, February 2007

Abbreviated title:

"A second-order continuity domain-decomposition technique"

*Corresponding author: Telephone +61 7 4631 1324, Fax +61 7 4631 2526, E-mail maiduy@usq.edu.au

Abstract This paper presents a second-order (instead of the usual first-order) continuity non-overlapping domain decomposition (DD) technique for numerically solving second-order elliptic problems in two-dimensional space. The proposed DD technique uses integrated Chebyshev polynomials to represent the solution in subdomains. The constants of integration are utilized to impose continuity of the second-order normal derivative of the solution at the interior points of subdomain interfaces. To also achieve a C^2 function at the intersection of interfaces, two additional unknowns are introduced at each intersection point. Numerical results show that the present domain decomposition method yields a higher level of accuracy than conventional DD techniques based on differentiated Chebyshev polynomials.

Keywords: Non-overlapping domain decomposition; Second-order continuity; Collocation point; Integrated Chebyshev polynomials; Second-order elliptic problems

1 Introduction

Domain decomposition techniques (cf. [1], [2]) are designed to deal with large-scale problems. The problem domain is decomposed into several subdomains, and each subdomain can be analyzed separately. A discretization method used for solving each subdomain is similar to that for a single domain. The use of subdomains facilitates an improvement in the condition number of the system matrix resulting from the discretization of the governing equation. For spectral methods, domain decompositions can also be used for the purpose of handling complex geometries. With the recent emergence of parallel computers, the DD techniques have become more attractive because they allow the parallel implementation of discretization schemes.

The basic part of any DD technique lies in the way employed to match the com-

puted solutions on contiguous regions. The choice between non-overlapping and overlapping subdomains has a profound effect on the computing strategy adopted.

In an overlapping domain technique, only continuity of the function is enforced. The interface solution is solved via an iterative procedure, in which nodal function values at interfaces are updated using previous approximate interior solutions of their neighbouring subdomain. The rate of convergence is an increasing function of the overlap.

In a non-overlapping domain method, continuity of the function and its normal derivative is imposed at selected points along the interfaces. The computed solution is thus considered to be C^1 continuous across the interfaces. For the case of many subdomains, there are further complications due to the presence of interior intersection points. There are two normal derivatives at an interior corner point, but one has only one equation to enforce their continuity. As a result, special treatment is required. Conventionally, one of these two normal derivatives is left out of the solution process [3].

Spectral methods (cf. [3], [4], [5]) have become increasingly popular in the computation of continuum mechanics problems. For smooth problems, they feature the property of spectral accuracy. In the context of pseudospectral techniques, given a tensor product grid, integrated Chebyshev polynomials were found to be more accurate than differentiated Chebyshev polynomials especially for the solution of high-order problems ([6], [7]).

In our previous work [8], a numerical scheme based on non-overlapping subdomains and integrated Chebyshev polynomials was presented in detail for the solution of one-dimensional elliptic problems. In the present work, the scheme is further developed for the case of two-dimensional elliptic problems with many subdomains. Particular emphasis is placed on the treatment for the difficulties in enforcing con-

tinuity conditions at the interior corner points (two equations, three unknowns). Karageorghis [9] proposed a fully conforming spectral collocation scheme, where the approximate solution is C^1 continuous not only at the interior points but also at both ends of the interfaces. Unlike DD techniques based on differential formulations (e.g. [3], [9], [10], [11]), the present integral DD technique achieves continuity in the second-order normal derivative of the solution everywhere on the interfaces.

An outline of the paper is as follows. A brief review of the integral collocation formulation using Chebyshev polynomials is given in Section 2. Section 3 describes the proposed DD technique based on integrated Chebyshev polynomials for second-order elliptic problems. Numerical results are presented in Section 4 to verify the formulation and to demonstrate the attractiveness of the proposed DD technique. Section 5 gives some concluding remarks.

2 The integral collocation formulation for single domains

For simplicity, the integral formulation is presented in detail through the solution of a Poisson equation

$$\nabla^2 u = b(x, y), \tag{1}$$

defined on a square domain $-1 \leq x, y \leq 1$ with Dirichlet boundary conditions.

Unlike conventional differential collocation formulations, the construction of the approximations for the field variable u here is based on integration. The second-order derivatives of the variable u are approximated using truncated Chebyshev series which are then integrated to obtain expressions for the first-order derivatives and the function itself.

The problem domain is discretized using a tensor product grid formed by the Gauss-Lobatto points

$$x_i = -\cos\left(\frac{(i-1)\pi}{N_x - 1}\right), \qquad i = 1, 2, \cdots, N_x \tag{2}$$

$$y_i = -\cos\left(\frac{(i-1)\pi}{N_y - 1}\right), \qquad i = 1, 2, \cdots, N_y. \tag{3}$$

Along a grid line that runs parallel to the $x-$axis, the variable u and its derivatives with respect to x are approximated by

$$\frac{\partial^2 u}{\partial x^2} = \sum_{k=1}^{N_x} a_k T_k(x) = \sum_{k=1}^{N_x} a_k I_k^{(2)}(x), \tag{4}$$

$$\frac{\partial u}{\partial x} = \sum_{k=1}^{N_x} a_k I_k^{(1)}(x) + c_1, \tag{5}$$

$$u = \sum_{k=1}^{N_x} a_k I_k^{(0)}(x) + c_1 x + c_2, \tag{6}$$

where $a_1, a_2, \cdots, a_{N_x}$ are expansion coefficients, c_1 and c_2 integration constants, $I_k^{(1)}(x) = \int I_k^{(2)}(x)dx$, $I_k^{(0)}(x) = \int I_k^{(1)}(x)dx$, and $T_k(x)$ or $I_k^{(2)}(x)$ the Chebyshev polynomial of the first kind defined as

$$T_k(x) = \cos((k-1)\arccos(x)). \tag{7}$$

To have the same unknown coefficient vector as (6), expressions (4) and (5) are rewritten as

$$\frac{\partial^2 u}{\partial x^2} = \sum_{k=1}^{N_x} a_k I_k^{(2)}(x) + c_1 0 + c_2 0, \tag{8}$$

$$\frac{\partial u}{\partial x} = \sum_{k=1}^{N_x} a_k I_k^{(1)}(x) + c_1 1 + c_2 0. \tag{9}$$

For two or higher dimensional problems, it would be more convenient to work in physical space than in spectral space. In currently used notations, $\widehat{\ }$ and $\widetilde{\ }$ denote

vectors/matrices that are associated with a grid line (one-dimensional domain) and the whole set of grid lines (two-dimensional domain), respectively.

Since (6) contains two extra coefficients c_1 and c_2, one can add two extra equations to the system that converts the spectral space into the physical space. These additional equations can be utilized to represent the values of $\partial u/\partial x$ and $\partial^2 u/\partial x^2$ at both ends of the line. The use of $\partial u/\partial x$ and $\partial^2 u/\partial x^2$ as extra information facilitates an effective implementation of Neumann boundary conditions and imposition of the differential equation on the boundaries, respectively. In the context of domain decompositions, it will be shown that satisfaction of the governing equation on the boundaries results in a C^2 solution across the interfaces. The conversion system for the case of using $\partial^2 u/\partial x^2$ is thus described in detail here

$$\widehat{\mathcal{C}} \begin{pmatrix} \widehat{a} \\ c_1 \\ c_2 \end{pmatrix} = \begin{pmatrix} \widehat{u} \\ \frac{\partial^2 u_1}{\partial x^2} \\ \frac{\partial^2 u_{Nx}}{\partial x^2} \end{pmatrix}, \tag{10}$$

where $\widehat{a} = (a_1, a_2, \cdots, a_{N_x})^T$, $\widehat{u} = (u_1, u_2, \cdots, u_{N_x})^T$, and $\widehat{\mathcal{C}}$ is the conversion matrix of dimension $(N_x + 2) \times (N_x + 2)$ defined as

$$\widehat{\mathcal{C}} = \begin{pmatrix} \widehat{\mathcal{H}} \\ \widehat{\mathcal{K}} \end{pmatrix}, \tag{11}$$

in which $\widehat{\mathcal{H}}$ and $\widehat{\mathcal{K}}$ are $N_x \times (N_x + 2)$ and $2 \times (N_x + 2)$ matrices that are constructed using (6) for $(x_1, x_2, \cdots, x_{N_x})$ and (8) for (x_1, x_{N_x}), respectively. Assume that $\widehat{\mathcal{C}}$ is invertible, solving (10) yields

$$\begin{pmatrix} \widehat{a} \\ c_1 \\ c_2 \end{pmatrix} = \widehat{\mathcal{C}}^{-1} \begin{pmatrix} \widehat{u} \\ \frac{\partial^2 u_1}{\partial x^2} \\ \frac{\partial^2 u_{Nx}}{\partial x^2} \end{pmatrix}. \tag{12}$$

Taking (12) into account, the evaluation of (8) and (9) at the grid points along an $x-$line yields

$$\widehat{\frac{\partial^k u}{\partial x^k}} = \widehat{\mathcal{D}}^{(kx)} \begin{pmatrix} \widehat{u} \\ \frac{\partial^2 u_1}{\partial x^2} \\ \frac{\partial^2 u_{N_x}}{\partial x^2} \end{pmatrix}, \qquad k = 1, 2, \tag{13}$$

where $\widehat{\frac{\partial^k u}{\partial x^k}} = \left(\frac{\partial^k u_1}{\partial x^k}, \frac{\partial^k u_2}{\partial x^k}, \cdots, \frac{\partial^k u_{N_x}}{\partial x^k} \right)^T$, and $\widehat{\mathcal{D}}^{(kx)} = \mathcal{I}^{(k)} \widehat{\mathcal{C}}^{-1}$ in which the matrices $\mathcal{I}^{(k)}$ are constructed via (9) for $k = 1$ and via (8) for $k = 2$ and they are of dimension $N_x \times (N_x + 2)$.

Expression (13) can be rewritten as

$$\widehat{\frac{\partial^k u}{\partial x^k}} = \widehat{\mathcal{D}}_1^{(kx)} \widehat{u} + \widehat{\mathcal{D}}_2^{(kx)} \begin{pmatrix} \frac{\partial^2 u_1}{\partial x^2} \\ \frac{\partial^2 u_{N_x}}{\partial x^2} \end{pmatrix}, \tag{14}$$

where $\widehat{\mathcal{D}}_1^{(kx)}$ and $\widehat{\mathcal{D}}_2^{(kx)}$ are the first N_x columns and the last two columns of the matrix $\widehat{\mathcal{D}}^{(kx)}$, respectively.

The Chebyshev approximations for $\partial^k u / \partial x^k$ $(k = 1, 2)$ over two-dimensional grids can be conveniently constructed by means of Kronecker tensor products [5]. Assume that the grid nodes are numbered from bottom to top and from left to right, the values of $\partial^k u / \partial x^k$ at the grid points will be computed by

$$\widetilde{\frac{\partial^k u}{\partial x^k}} = \widetilde{\mathcal{D}}^{(kx)} \widetilde{u} + \widetilde{l}^{(kx)}, \tag{15}$$

where

$$\widetilde{\frac{\partial^k u}{\partial x^k}} = \left(\frac{\partial^k u_1}{\partial x^k}, \frac{\partial^k u_2}{\partial x^k}, \cdots, \frac{\partial^k u_{N_x N_y}}{\partial x^k} \right)^T, \tag{16}$$

$$\widetilde{u} = (u_1, u_2, \cdots, u_{N_x N_y})^T, \tag{17}$$

$$\widetilde{\mathcal{D}}^{(kx)} = \widehat{\mathcal{D}}_1^{(kx)} \otimes \widetilde{\mathbf{1}}, \tag{18}$$

$$\widetilde{l}^{(kx)} = \left(\widehat{\mathcal{D}}_2^{(kx)} \otimes \widehat{\mathbf{1}} \right) \cdot \left(\widehat{\mathbf{1}} \otimes \left[\left(\widehat{\frac{\partial^2 u}{\partial x^2}} \right)_L, \left(\widehat{\frac{\partial^2 u}{\partial x^2}} \right)_R \right] \right), \tag{19}$$

in which $\otimes$ denotes the Kronecker tensor product, $\cdot$ the element-by-element product of two matrices, $\widetilde{\mathbf{1}}$ the unit matrix of dimension $N_y \times N_y$, $\widehat{\mathbf{1}}$ the $N_x \times 1$ vector of all ones, $\left(\widehat{\frac{\partial^2 u}{\partial x^2}}\right)_L$ and $\left(\widehat{\frac{\partial^2 u}{\partial x^2}}\right)_R$ the vectors of values of $\frac{\partial^2 u}{\partial x^2}$ along the left and right sides of the domain. It is straightforward to compute the two vectors $\left(\widehat{\frac{\partial^2 u}{\partial x^2}}\right)_L$ and $\left(\widehat{\frac{\partial^2 u}{\partial x^2}}\right)_R$ using the following relation

$$\frac{\partial^2 u}{\partial x^2} = b - \frac{\partial^2 u}{\partial y^2}. \tag{20}$$

and hence $\widetilde{l}^{(kx)}$ are known vectors.

In a similar way, one finds the Chebyshev approximations for the first- and second-order derivatives of u with respect to y. The values of u at the interior points are determined by solving the following determinate system of algebraic equations

$$\widetilde{\mathcal{A}}_{(ip,ip)} \widetilde{u}_{(ip)} = \widetilde{f}_{(ip)}, \tag{21}$$

where

$$\widetilde{\mathcal{A}}_{(ip,ip)} = \widetilde{D}^{(2x)}_{(ip,ip)} + \widetilde{D}^{(2y)}_{(ip,ip)}, \tag{22}$$

$$\widetilde{f}_{(ip)} = \widetilde{b}_{(ip)} - \widetilde{l}^{(2x)}_{(ip)} - \widetilde{l}^{(2y)}_{(ip)} - \widetilde{\mathcal{A}}_{(ip,bp)} \widetilde{u}_{(bp)}, \tag{23}$$

in which bp and ip denote the boundary and interior points, respectively.

3 The proposed domain-decomposition technique

The problem domain can be irregular to the extent that it can be domain-decomposed into a number of regular domains where the use of tensor product grids is feasible. The solution procedure of a substructuring technique involves two main steps: (i) Find the solution on subdomain interfaces and (ii) Find the solution in subdomains. The present substructuring technique is based on the use of integrated Chebyshev polynomials to represent approximate solutions in subdomains. It provides a C^2 continuity of the approximate solution across the interfaces. The method is first presented for the simplest case of two subdomains, and then extended to the case of multiple subdomains.

3.1 Two subdomains

A simple domain decomposition for a rectangular domain is illustrated in Figure 1. On the interface Γ between two subdomains I and II, one can choose unknown values in the form of a Dirichlet-Dirichlet type or a Neumann-Dirichlet type. The present work employs the Dirichlet-Dirichlet type

$$u_k^I = u_k^{II} = u_k^\Gamma, \qquad k = \{2, 3, \cdots, N_y - 1\}. \tag{24}$$

These unknowns $\{u_k^\Gamma\}_{k=2}^{N_y-1}$ will be determined by matching the first-order normal derivative of u at the interface Γ

$$\left(\frac{\partial u_k}{\partial x}\right)^I = \left(\frac{\partial u_k}{\partial x}\right)^{II}, \qquad k = \{2, 3, \cdots, N_y - 1\}. \tag{25}$$

Let fp denote the interior points on Γ. To form the interface system (25) (the so-called Schur complement system), one needs to compute the vector $\left(\widetilde{\frac{\partial u}{\partial x}}\right)$ associated

with each of two subdomains at fp in terms of nodal boundary values of u (i.e. $\widetilde{u}_{(bp)}$).

Using (15), the values of $\partial u/\partial x$ along Γ are computed by

$$\left(\widetilde{\frac{\partial u}{\partial x}}\right)_{(fp)} = \widetilde{D}^{(1x)}_{(fp,bp)}\widetilde{u}_{(bp)} + \widetilde{D}^{(1x)}_{(fp,ip)}\widetilde{u}_{(ip)} + \widetilde{l}^{(1x)}_{(fp)}. \tag{26}$$

Taking (21) into account, the second term on the right-hand side of (26) is replaced with

$$\widetilde{D}^{(1x)}_{(fp,ip)}\widetilde{u}_{(ip)} = -\widetilde{D}^{(1x)}_{(fp,ip)}\widetilde{\mathcal{A}}^{-1}_{(ip,ip)}\widetilde{\mathcal{A}}_{(ip,bp)}\widetilde{u}_{(bp)} + \widetilde{D}^{(1x)}_{(fp,ip)}\widetilde{\mathcal{A}}^{-1}_{(ip,ip)}\left(\widetilde{b}_{(ip)} - \widetilde{l}^{(2x)}_{(ip)} - \widetilde{l}^{(2y)}_{(ip)}\right). \tag{27}$$

In (26) and (27), there remain three terms, namely $\widetilde{l}^{(1x)}_{(fp)}, \widetilde{l}^{(2x)}_{(ip)}$ and $\widetilde{l}^{(2y)}_{(ip)}$, which contain the values of

$$\left(b - \partial^2 u/\partial t^2\right) \tag{28}$$

($t-$ is the direction tangent to a local boundary) at the interior points on the four sides of each subdomain. These values are known on the three actual boundaries, but unknown on the interface Γ. The following are two approaches proposed for the approximation of $\partial^2 u/\partial t^2$ on Γ

3.1.1 Approach 1

This approach uses differential collocation formulations and hence one can have

$$\widehat{\frac{\partial^2 u}{\partial t^2}} = \widehat{\frac{\partial^2 u}{\partial y^2}} = \mathbf{D}^2\widehat{u} = \mathbf{D}^2\begin{pmatrix} u^{\Gamma}_1 \\ u^{\Gamma}_2 \\ \cdots \\ u^{\Gamma}_{N_y} \end{pmatrix}, \tag{29}$$

where $\mathbf{D}$ is the differentiation matrix whose entries are explicitly known (see, e.g., [3], [4], [5]).

3.1.2 Approach 2

This approach is based on the integral collocation formulation

$$\widehat{\frac{\partial^2 u}{\partial t^2}} = \widehat{\frac{\partial^2 u}{\partial y^2}} = \widehat{\mathcal{D}}^{(2y)} \begin{pmatrix} \widehat{u} \\ \frac{\partial^2 u_1}{\partial y^2} \\ \frac{\partial^2 u_{N_y}}{\partial y^2} \end{pmatrix} = \widehat{\mathcal{D}}^{(2y)} \begin{pmatrix} u_1^\Gamma \\ u_2^\Gamma \\ \cdots \\ u_{N_y}^\Gamma \\ \frac{\partial^2 u_1^\Gamma}{\partial y^2} \\ \frac{\partial^2 u_{N_y}^\Gamma}{\partial y^2} \end{pmatrix}, \tag{30}$$

in which the values of $\partial^2 u_1^\Gamma / \partial y^2$ and $\partial^2 u_{N_y}^\Gamma / \partial y^2$ are easily obtained using (1).

For calculating the values of $\partial^2 u / \partial t^2$ at the interior point on Γ, the first and last rows of $\mathbf{D}^2$ in (29) and of $\widehat{\mathcal{D}}^{(2y)}$ in (30) are removed.

It can be seen that the two vectors $\left(\widetilde{\frac{\partial u}{\partial x}}\right)^I_{(fp)}$ and $\left(\widetilde{\frac{\partial u}{\partial x}}\right)^{II}_{(fp)}$ are now written in terms of nodal boundary values of u. By substituting them into (25) and then imposing Dirichlet boundary conditions, one obtains a determinate system of equations for the interface unknown vector $\widetilde{u}_{fp} = \left(u_2^\Gamma, u_3^\Gamma, \cdots, u_{N_y-1}^\Gamma\right)^T$. Once this vector is found, it is straightforward to obtain the solution in subdomains by using (21).

3.1.3 A C^2 solution across the interface

From the above process, i.e. (24), (25), (10) and (20), the following constraints are imposed at the interior points on the interface Γ

$$u_k^I = u_k^{II}, \tag{31}$$

$$\left(\frac{\partial u_k}{\partial x}\right)^I = \left(\frac{\partial u_k}{\partial x}\right)^{II}, \tag{32}$$

$$\left(\frac{\partial^2 u_k}{\partial x^2}\right)^I = b_k^I - \left(\frac{\partial^2 u_k}{\partial y^2}\right)^I, \tag{33}$$

$$\left(\frac{\partial^2 u_k}{\partial x^2}\right)^{II} = b_k^{II} - \left(\frac{\partial^2 u_k}{\partial y^2}\right)^{II}, \tag{34}$$

where $k = 2, 3, \cdots, N_y - 1$.

Consider (33) and (34). Approximations for $\left(\frac{\partial^2 u}{\partial y^2}\right)^I$ and $\left(\frac{\partial^2 u}{\partial y^2}\right)^{II}$ along the interface Γ are identical because they are based on the same information. On the other hand, one also has $b_k^I = b_k^{II}$. The two equations (33) and (34) thus lead to

$$\left(\frac{\partial^2 u_k}{\partial x^2}\right)^I = \left(\frac{\partial^2 u_k}{\partial x^2}\right)^{II}, \qquad k = 2, 3, \cdots, N_y - 1. \tag{35}$$

Hence, equations (31), (32) and (35) indicate that the present DD technique provides a C^2 solution across the interface Γ.

3.2 Multiple subdomains

The solution procedure for the case of two subdomains is now extended to the case of multiple subdomains. Special attention needs to be paid to the treatment for continuity conditions at the interior corner points.

It can be seen from (29), Approach 1 introduces the values of u at both ends of a line.

In the case of many subdomains, this approach thus produces one unknown value at each interior corner point, and correspondingly one needs to add one additional equation to the interface system. Possible choices for this equation include

$$\left(\frac{\partial u}{\partial x}\right)_L = \left(\frac{\partial u}{\partial x}\right)_R, \tag{36}$$

$$\left(\frac{\partial u}{\partial y}\right)_B = \left(\frac{\partial u}{\partial y}\right)_T, \tag{37}$$

$$\frac{1}{2}\left(\left(\frac{\partial^2 u}{\partial x^2}\right)_L + \left(\frac{\partial^2 u}{\partial x^2}\right)_R\right) + \frac{1}{2}\left(\left(\frac{\partial^2 u}{\partial y^2}\right)_B + \left(\frac{\partial^2 u}{\partial y^2}\right)_T\right) = b, \tag{38}$$

where L, R, B, T stand for left, right, bottom and top of the interior corner point, respectively. Among them, it can be seen that only (38) uses information from both $x-$ and $y-$ directions. To investigate the effect of continuity order of the approximate solution at the interior corner points, (38) is chosen here. The computed solution is seen to be C^2 continuous at the interior points on the interfaces and "C^0 continuous" at the interior corner points.

For Approach 2, there are three values ($u, \partial^2 u/\partial x^2$ and $\partial^2 u/\partial y^2$) at each interior corner point as shown in (30). To achieve a C^2 solution at an interior corner point, the basic idea here is to also consider the values of $\partial^2 u/\partial x^2$ and $\partial^2 u/\partial y^2$ as two additional unknowns. Since the number of unknowns becomes greater (3 instead of 1), one can add the following three independent equations

$$\left(\frac{\partial u}{\partial x}\right)_L = \left(\frac{\partial u}{\partial x}\right)_R, \tag{39}$$

$$\left(\frac{\partial u}{\partial y}\right)_B = \left(\frac{\partial u}{\partial y}\right)_T, \tag{40}$$

$$\frac{\partial^2 u}{\partial x^2} + \frac{\partial^2 u}{\partial y^2} = b, \tag{41}$$

to the interface system. In other words, the solution u and its second-order derivatives in the $x-$ and $y-$ directions are required to be continuous, while the first-order derivatives $\partial u/\partial x$ and $\partial u/\partial y$ are forced to match at the interior corner point. It

can be seen this treatment provides a C^2 solution at the interior corner points. The accuracy of Approach 2 is expected to be better than that of Approach 1.

For problems with Neumann boundary conditions, a slight modification for the conversion process is required. The extra equation at a point on the actual boundary is utilized to implement a normal derivative boundary condition. Since the normal derivative $\partial u/\partial n$ ($n-$the direction normal to the local boundary) is prescribed along the boundary, this equation does not introduce any new unknowns. The other extra equation at a point on the interface is employed as before and hence continuity of the second-order derivatives of u across the interface is maintained.

4 Numerical results

The grid size is defined as the minimum of average distances between the grid points in the $x-$ and $y-$directions

$$h = \min\left\{L_x/(N_x-1), L_y/(N_y-1)\right\}, \tag{42}$$

where L is the length of the side and N is the total number of points. The accuracy of a numerical solution is measured via a discrete relative L_2 error

$$N_e(f) = \sqrt{\frac{\sum_{i=1}^{M}\left(f_i^{(e)} - f_i^{(a)}\right)^2}{\sum_{i=1}^{M}\left(f_i^{(e)}\right)^2}}, \tag{43}$$

where M is the total number of collocation points, and $f^{(e)}$ and $f^{(a)}$ the exact and approximate solutions, respectively.

4.1 Function approximation

This section is concerned with a special class of function approximation. Apart from a given set of function nodal values, one also knows some nodal values of its derivatives. In this case, the use of the integral formulation can enhance the quality of the function approximation. This is demonstrated through the calculation of first- and second-order derivatives of the following function

$$y = \sin(x), \quad -1 \leq x \leq 1, \tag{44}$$

where the values of y at the whole set of grid points and the values of d^2y/dx^2 at the two boundary points are given. The numerical schemes used here are similar to those described in Approach 1 and Approach 2, respectively. In determining expansion coefficients, conventional differential formulations use the set of function values only, while the integral formulation takes all information into account. Results concerning $N_e(dy/dx)$ and $N_e(d^2y/dx^2)$ are shown in Figure 2. Both formulations employ the same sets of grid points. It can be seen that the integral formulation yields a higher degree of accuracy than the differential one.

4.2 Partial differential equations

The present DD technique is verified through the solution of the following Poisson equation

$$\nabla^2 u = 4(1-\pi^2)\left[\sin(2\pi x)\cosh(2y) - \cos(2\pi x)\sinh(2y)\right], \tag{45}$$

defined on the square $-1 \leq x, y \leq 1$, subject to Dirichlet boundary conditions

$$u = -\sinh(2y), \qquad x = \pm 1, \tag{46}$$

$$u = \sin(2\pi x)\cosh(\pm 2) - \cos(2\pi x)\sinh(\pm 2), \qquad y = \pm 1. \tag{47}$$

The exact solution of (45)-(47) can be verified to be

$$u = \sin(2\pi x)\cosh(2y) - \cos(2\pi x)\sinh(2y), \tag{48}$$

which is depicted in Figure 3.

The problem domain is divided into 2, 4, 9, 16, 25, 36 and 49 subdomains. For a fixed number of subdomains, various tensor product grids are employed to study the convergence behaviour of the method.

4.2.1 Comparison with conventional differential DD techniques

To assess the performance of the present integral DD technique, the obtained results are compared with those of conventional differential DD techniques. It is noted that conventional techniques yield only a C^1 solution across the interfaces; the solution procedure used here is similar to that described in [3]. Figures 4 and 5 show plots of $N_e(u)$ versus h. For a fixed number of subdomains, it can be seen that both techniques yield spectral accuracy and the accuracy of Approach 1 (legend "Integral(1)") and Approach 2 ("Integral(2)") is superior to that of the conventional one ("Differential").

To study the influence of the C^2 condition on the solution accuracy, the case of a single domain is also considered here. It can be seen from Figures 4 and 5, the gaps between two curves for the domain-decomposition case (legends "Differential"

and "Integral(2)") are much wider than that for the single domain case (legends "Differential" and "Integral"). If one takes results obtained by the differential formulation as the basis, the integral formulation is seen to perform much better for the case of multiple subdomains than for the case of a single domain. It thus appears that the achievement of a C^2 solution across the interfaces results in a significant improvement in accuracy.

4.2.2 Comparison of the performance of the integral DD technique between Approach 1 and Approach 2

The main difference between Approach 1 and Approach 2 is that a second-order continuity of the solution is achieved at every point on the interfaces for the latter, but only at the interior points on the interfaces for the former.

For the case of 2 subdomains, there are no interior corner points. Numerical results show that the performance of Approach 2 is similar to that of Approach 1 despite the fact that the former yields more accurate results than the latter for function approximation (Section 4.1). From Figure 4, there is no discernible difference of $N_e(u)$ between the two approaches.

For the case of 4 subdomains, there is only one interior corner point. The performance of Approach 2 is slightly better than that of Approach 1. However, it is still difficult to see the gap between two curves from the plot (Figure 4).

For the case of 9 subdomains and more, a number of interior corner points become noticeable. Approach 2 is found to be more accurate than Approach 1 by about two orders of magnitude.

These observations indicate that the continuity order of the solution at the intersec-

tion points strongly affects the accuracy of the integral DD technique which is always better than differential DD techniques. Approach 2 is recommended for practical use.

5 Concluding remarks

In this paper, a domain decomposition technique which provides a C^2, instead of the usual C^1, solution for second-order elliptic problems is reported. This achievement of higher-order smoothness is due to satisfaction of the governing equation on the boundaries. Two approaches are proposed and studied in detail. The first approach satisfies a C^2 condition of the solution at the interior points on the interfaces and C^0 at the interior corner points, while the second approach provides a C^2 solution at every point on the interfaces. Numerical results obtained show that

(i) both approaches outperform conventional DD techniques regarding accuracy, and

(ii) the performance of the second approach is far superior to that of the first approach.

Acknowledgements

This research was supported by the Australian Research Council.

References

1. A. Quarteroni and A. Valli, *Domain Decomposition Methods for Partial Differential Equations*, Clarendon Press, Oxford, 1999.

2. B.F. Smith, P.E. Bjorstad and W.D. Gropp, *Domain Decomposition Parallel Multilevel Methods for Elliptic Partial Differential Equations*, Cambridge University Press, New York, 1996.

3. C. Canuto, M.Y. Hussaini, A. Quarteroni and T.A. Zang, *Spectral Methods in Fluid Dynamics*, Springer-Verlag, New York, 1988.

4. B. Fornberg, *A Practical Guide to Pseudospectral Methods*, Cambridge University Press, Cambridge, 1998.

5. L.N. Trefethen, *Spectral Methods in MATLAB*, SIAM, Philadelphia, 2000.

6. N. Mai-Duy, An effective spectral collocation method for the direct solution of high-order ODEs, *Communications in Numerical Methods in Engineering* **22**(6) (2006) 627–642.

7. N. Mai-Duy and R.I. Tanner, A spectral collocation method based on integrated Chebyshev polynomials for biharmonic boundary-value problems, *Journal of Computational and Applied Mathematics* **201**(1) (2007) 30–47.

8. N. Mai-Duy and T. Tran-Cong, An efficient domain-decomposition pseudo-spectral method for solving elliptic differential equations, *Communications in Numerical Methods in Engineering*, accepted.

9. A. Karageorghis, A fully conforming spectral collocation scheme for second- and fourth-order problems, *Computer Methods in Applied Mechanics and Engineering* **126** (1995) 305–314.

10. A. Karageorghis, Conforming Chebyshev spectral methods for Poisson problems in rectangular domains, *Journal of Scientific Computing* **8**(2) (1993) 123–133.

11. D. Funaro, A. Quarteroni and P. Zanolli, An iterative procedure with interface relaxation for domain decomposition methods, *SIAM Journal of Numerical Analysis* **25**(6) (1988) 1213–1236.

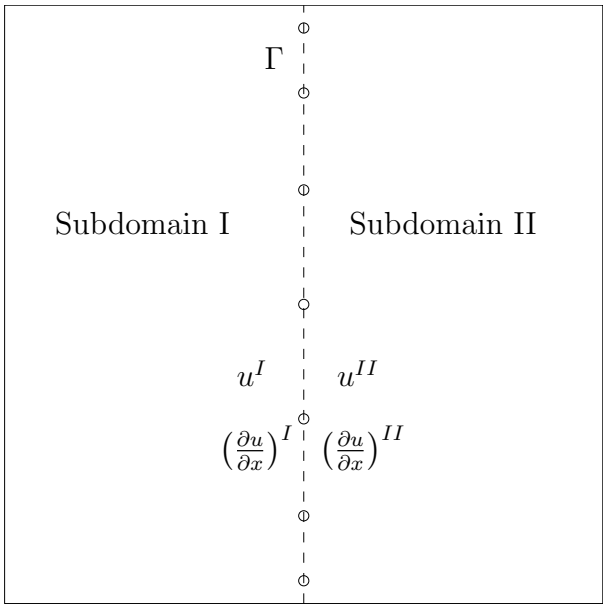

Figure 1: Two subdomains. The symbol ∘ denotes the interior points on the interface Γ.

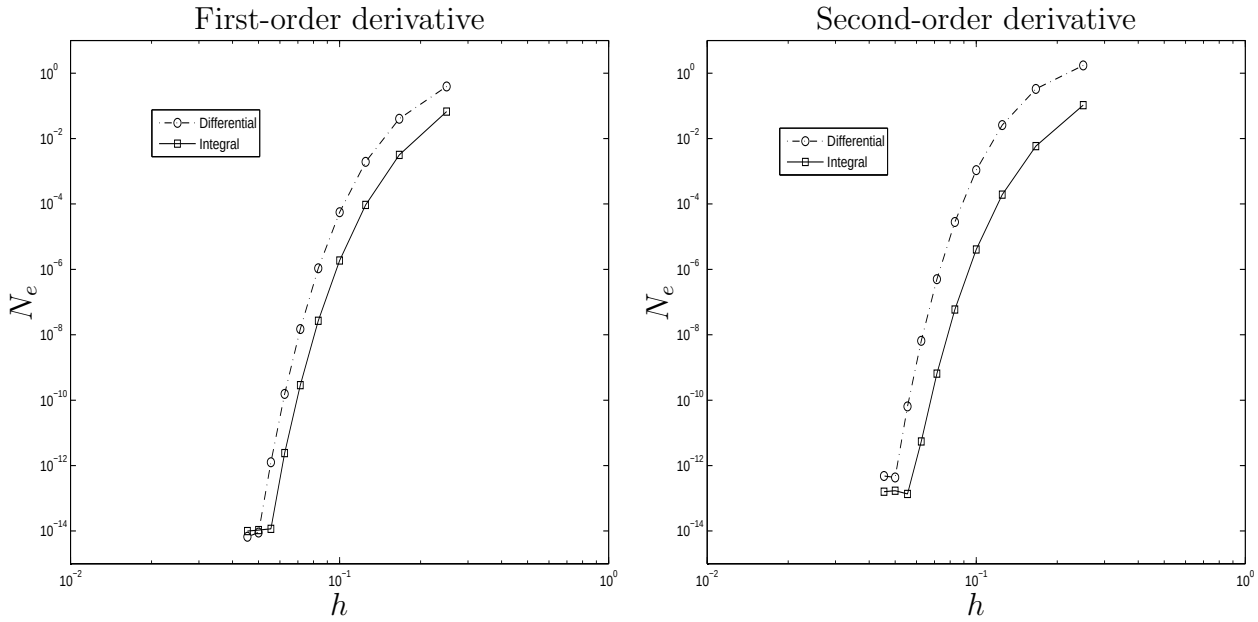

Figure 2: Function approximation, $y = \sin(x), -1 \leq x \leq 1$. Comparison of accuracy between the differential and integral formulations. All plots have the same axis scaling.

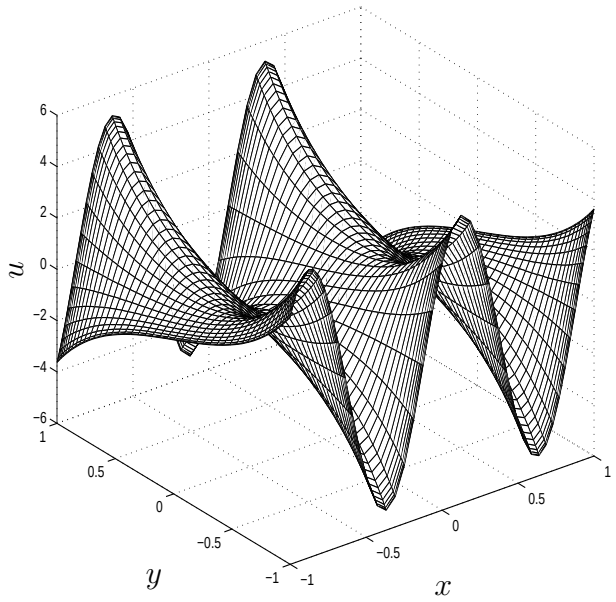

Figure 3: Poisson equation, the exact solution.

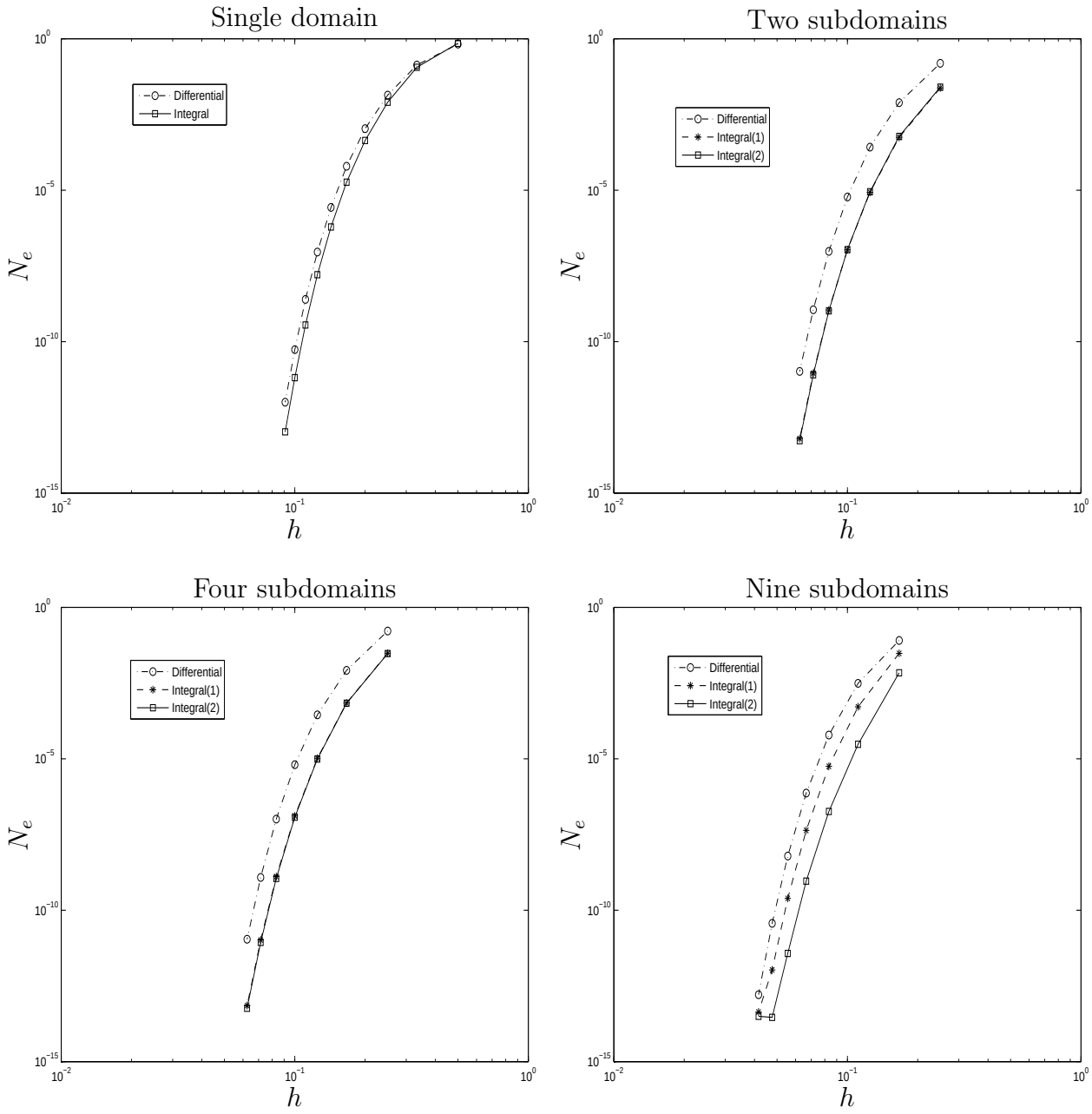

Figure 4: Poisson equation. For each case, a number of tensor product grids, namely $5 \times 5, 7 \times 7, \cdots, 17 \times 17$, are employed. For the case of two subdomains, there is no discernible difference of N_e between Integral(1) (Approach 1) and Integral(2) (Approach 2). All plots have the same axis scaling.

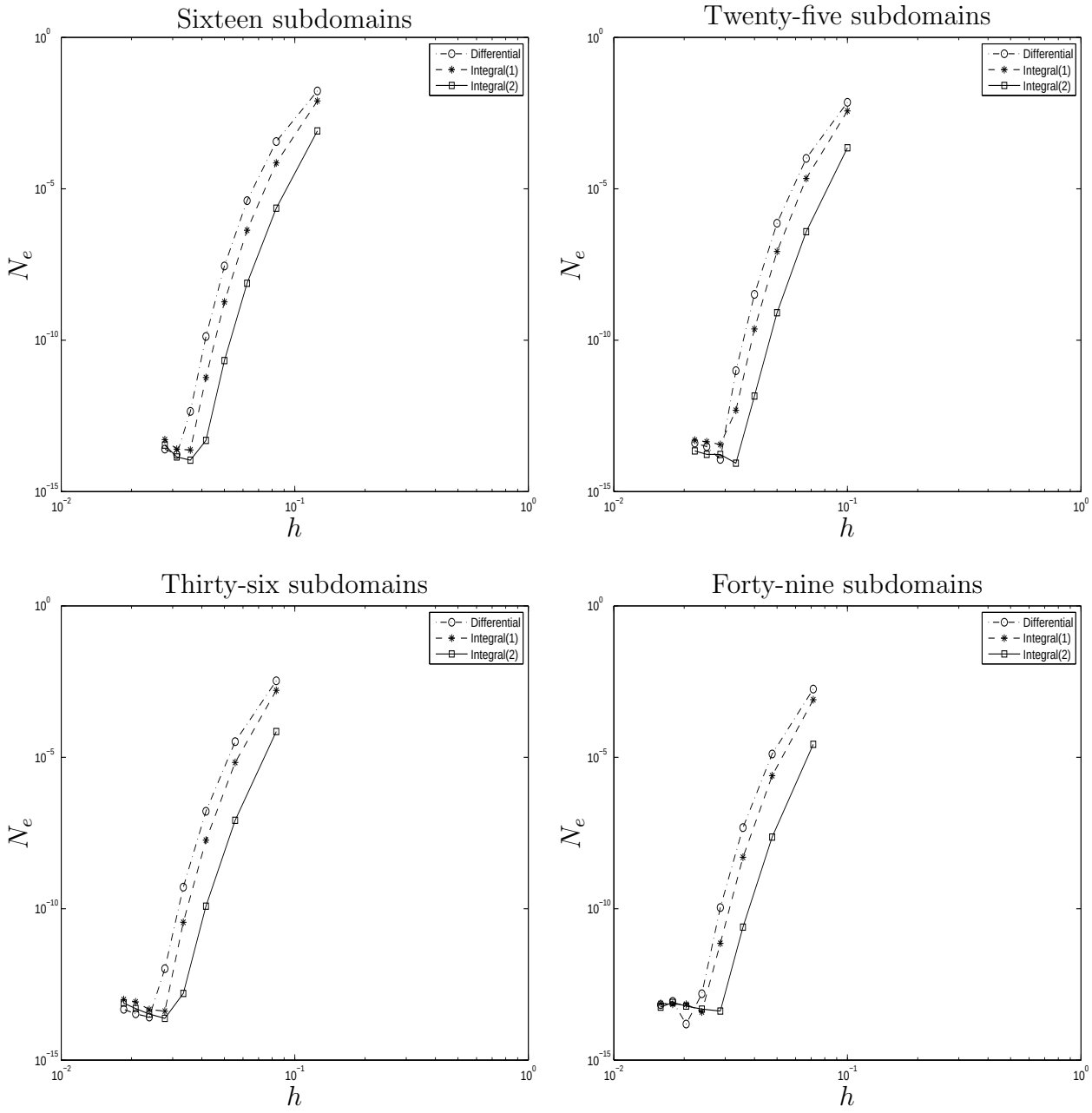

Figure 5: Poisson equation. For each case, a number of tensor product grids, namely $5 \times 5, 7 \times 7, \cdots, 19 \times 19$, are employed. All plots have the same axis scaling.